NUSC Technical Report 6738
1 December 1988

Transition to Turbulence in Constant-Acceleration Pipe Flow

P. J. Lefebvre
Launcher & Missile Systems Department

Naval Underwater Systems Center
Newport, Rhode Island / New London, Connecticut

PREFACE

This report was prepared under NUSC IR-IED Project No. A43100, "Transition in Accelerating Flows," principal investigator P.J. Lefebvre (Code 8322).

The technical reviewer for this report was K.M. LaPointe (Code 8322).

The author wishes to express his appreciation to K.M. LaPointe (Code 8322) for his assistance in conducting the tests on the 5-cm-diameter test section, to J. Brown (Code 8322) for his assistance in conducting the 9-cm-diameter test section experiments and for data reduction, and to R. Waclawik (Code 8322) for his efforts in designing and overseeing installation of the 9-cm-diameter test section and the associated control valve section.

REVIEWED AND APPROVED: 1 DECEMBER 1988

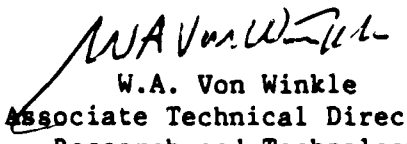

W.A. Von Winkle
Associate Technical Director,
Research and Technology

REPORT DOCUMENTATION PAGE

1a. REPORT SECURITY CLASSIFICATION UNCLASSIFIED	1b. RESTRICTIVE MARKINGS
2a. SECURITY CLASSIFICATION AUTHORITY	3. DISTRIBUTION / AVAILABILITY OF REPORT Approved for public release; distribution unlimited.
2b. DECLASSIFICATION / DOWNGRADING SCHEDULE	
4. PERFORMING ORGANIZATION REPORT NUMBER(S) TR 6738	5. MONITORING ORGANIZATION REPORT NUMBER(S)
6a. NAME OF PERFORMING ORGANIZATION Naval Underwater Systems Ctr 6b. OFFICE SYMBOL (If applicable) Code 8322	7a. NAME OF MONITORING ORGANIZATION
6c. ADDRESS (City, State, and ZIP Code) Newport Laboratory Newport, RI 02841	7b. ADDRESS (City, State, and ZIP Code)
8a. NAME OF FUNDING / SPONSORING ORGANIZATION 8b. OFFICE SYMBOL (If applicable)	9. PROCUREMENT INSTRUMENT IDENTIFICATION NUMBER
8c. ADDRESS (City, State, and ZIP Code)	10. SOURCE OF FUNDING NUMBERS PROGRAM ELEMENT NO. / PROJECT NO. / TASK NO. / WORK UNIT ACCESSION NO

11. TITLE (Include Security Classification)
TRANSITION TO TURBULENCE IN CONSTANT-ACCELERATION PIPE FLOW

12. PERSONAL AUTHOR(S)
Lefebvre, P.J.

13a. TYPE OF REPORT	13b. TIME COVERED FROM ____ TO ____	14. DATE OF REPORT (Year, Month, Day)	15. PAGE COUNT
Final		88-12-01	35

16. SUPPLEMENTARY NOTATION

17. COSATI CODES		
FIELD	GROUP	SUB-GROUP
20	04	

18. SUBJECT TERMS (Continue on reverse if necessary and identify by block number)
Fluid Mechanics ,
Accelerating Pipe Flow . (mgw)

19. ABSTRACT (Continue on reverse if necessary and identify by block number)

The purpose of this report is to present results from the second Naval Underwater Systems Center project on accelerating flows. The main objectives of this second project were to investigate the details of the transition process and to validate the transition correlation parameters developed under the first project. The details of the transition process were investigated using the existing 5-cm-diameter test section, but with one axial location supplemented with additional wall shear stress sensors in an effort to detect the propagation of turbulence. Validation of the previously developed transition correlation parameters was accomplished by conducting constant-acceleration experiments on a new and larger 9-cm-diameter test section. Additionally, transition for mean accelerations lower than those tested previously was investigated on the 9-cm-diameter test section.

20. DISTRIBUTION / AVAILABILITY OF ABSTRACT ☐ UNCLASSIFIED/UNLIMITED ☒ SAME AS RPT ☐ DTIC USERS	21. ABSTRACT SECURITY CLASSIFICATION UNCLASSIFIED
22a. NAME OF RESPONSIBLE INDIVIDUAL P.J. Lefebvre	22b. TELEPHONE (Include Area Code) (401) 841-1905 22c. OFFICE SYMBOL Code 8322

DD FORM 1473, 84 MAR 83 APR edition may be used until exhausted.
All other editions are obsolete.

TABLE OF CONTENTS

LIST OF ILLUSTRATIONS

LIST OF SYMBOLS

D	Test section diameter
dP/dx	Axial pressure gradient
J_0	Bessel function of the first kind
K	Convective acceleration parameter
K_a	Local acceleration parameter
$K_{a,tr}$	Local acceleration parameter at transition
P	Pressure
R	Pipe radius
Re_D	Pipe Reynolds number
Re_{tr}	Reynolds number at transition
Re_δ	Boundary layer thickness Reynolds number
r	Radial distance from pipe centerline
r^*	Dimensionless radial position = r/R
T	Fluid temperature in °C
t	Time
t^*	Dimensionless time = $\upsilon t/R^2$
t_{tr}	Time to transition from $t = 0$
t^*_{tr}	Dimensionless time at transition, from start of transition
U	Instantaneous local axial velocity
$\bar{U}$	Time-mean local axial velocity
U_{cl}	Instantaneous centerline velocity
$\bar{U}_m$	Time-mean cross-sectional averaged velocity
U_m	Instantaneous cross-sectional averaged velocity
U_{max}	Steady-state centerline velocity
$\bar{U}_{mf}$	Final time-mean cross-sectional averaged velocity
$U_{m,tr}$	Cross-sectional averaged velocity at transition
$\ddot{X}$	Average acceleration during test run
x	Axial distance
Y	Distance from wall
δ	Boundary layer thickness
δ_{tr}	Boundary layer thickness at transition
λ_N	Roots of the Bessel function
μ	Dynamic viscosity
ρ	Mass density
τ_w	Instantaneous wall shear stress
υ	Kinematic viscosity

TRANSITION TO TURBULENCE IN CONSTANT-ACCELERATION PIPE FLOW

INTRODUCTION

Accelerating shear flows and other time-dependent laminar and turbulent shear flows are encountered in many aerodynamic and hydrodynamic applications. Examples include the startup of a closed-conduit flow, a train rapidly entering a tunnel, flow over turbine blades, submarine and aircraft maneuverings, and the highly transient launch of a torpedo.

Even in simple geometries such as circular pipes, the complex nature of unsteady laminar, turbulent, and transitional flow have proven to be very difficult to characterize experimentally or solve analytically. Relatively little theoretical or numerical work has been directed at this problem.

Only recently have any detailed experiments been conducted on the physics of accelerating flows. The most comprehensive study was a previous Naval Underwater Systems Center (NUSC) project, which was conducted over a 3-year period concluding in FY 1987 and reported in reference 1. This was the first unsteady flow experiment of its kind conducted at NUSC.

All tests of that project were conducted in the NUSC Unsteady Flow Loop Facility, which was developed and built coincident with the project and funded mainly with NUSC capital asset funds. This facility is capable of providing user-programmed acceleration of the mean flow over a large range of velocities and accelerations. Details of this facility are provided in reference 2.

The first unsteady flow study (reference 1) used a 5-cm-diameter circular test section and evaluated the effect of the constant acceleration of the mean flow on many of the prevalent flow parameters including: (1) time-dependent velocity profiles and turbulence intensity for accelerations starting from rest and from an initially turbulent flow, (2) transient wall shear stress, and (3) time of and conditions for transition from laminar to turbulent flow.

Earlier experimental studies by others have been limited in the types of unsteady flow investigated. In general, these past experiments have investigated either pulsating flow (references 3, 4, and 5), a suddenly applied constant pressure gradient (references 6 and 7), or a suddenly applied stepwise change in flow rate (references 8, 9, and 10). In short, these earlier experimental studies have been largely limited to low pipe Reynolds numbers and in the flow conditions studied and the types of data acquired. Because acceleration and the time rate of change of acceleration changed continuously over any one run, results were essentially applicable only to the specific cases studied.

The purpose of this report is to present results from the second NUSC project on accelerating flows, which was conducted during FY 1988. The main objectives of this second project were to investigate the details of the transition process and to validate the transition correlation parameters developed under the first project.

The details of the transition process were investigated using the existing 5-cm-diameter test section, but with one axial location supplemented with additional wall shear stress sensors in an effort to detect the propagation of turbulence. Validation of the previously developed transition correlation parameters was accomplished by conducting constant acceleration experiments on a new and larger 9-cm-diameter test section. Additionally, transition for mean accelerations lower than those tested previously (i.e., less than 1.8 m/sec^2) was investigated on the 9-cm-diameter test section.

EXPERIMENTAL FACILITY AND INSTRUMENTATION

The Unsteady Flow Loop Facility is located at the NUSC Newport Laboratory. The design operation and specifics of this experimental facility are described in detail in reference 2. A general overview of the physical configuration and the transient flow instrumentation is given in the following paragraphs.

The layout of the test facility is shown in figure 1. A stainless steel reservoir supplies a 150-hp pump, which delivers flow to the test section. Vibration and noise isolators, along with flow straighteners and conditioners, are provided where appropriate. A control valve installed downstream of the test section is part of the feedback control system that provides programmed acceleration of the flow. Reservoir water is conditioned to maintain its temperature to within $\pm 1°C$, and filters remove particles as small as 0.5 micron. The test section flow rate is monitored to within ± 1.0 percent of reading by a transient electromagnetic flowmeter, whose details are described in reference 11. This flowmeter was developed as part of the flow loop facility design project since there are no other known commercially available flowmeters that have the capability of making accurate transient measurements.

Figure 2 shows the 5-cm-diameter test section on which the first project was conducted. This test section was slightly modified for the first phase of the present tests. The test section consists of six 5-m-long stainless steel circular sections followed by a 30-cm cast acrylic circular section through which laser Doppler velocimeter (LDV) measurements are made. There is a sensor station placed at the end of the six stainless steel sections, each of which consists of a static pressure tap, a flush-mounted wall pressure sensor, and a hot-film wall shear stress sensor. These sensor stations are spaced 5-m apart.

For the present series of experiments, the acrylic test section was fitted with four hot-film wall shear stress sensors positioned near the LDV axial measurement station as shown in figure 2. The intent of the instrumented acrylic section was to investigate the direction of propagation of the

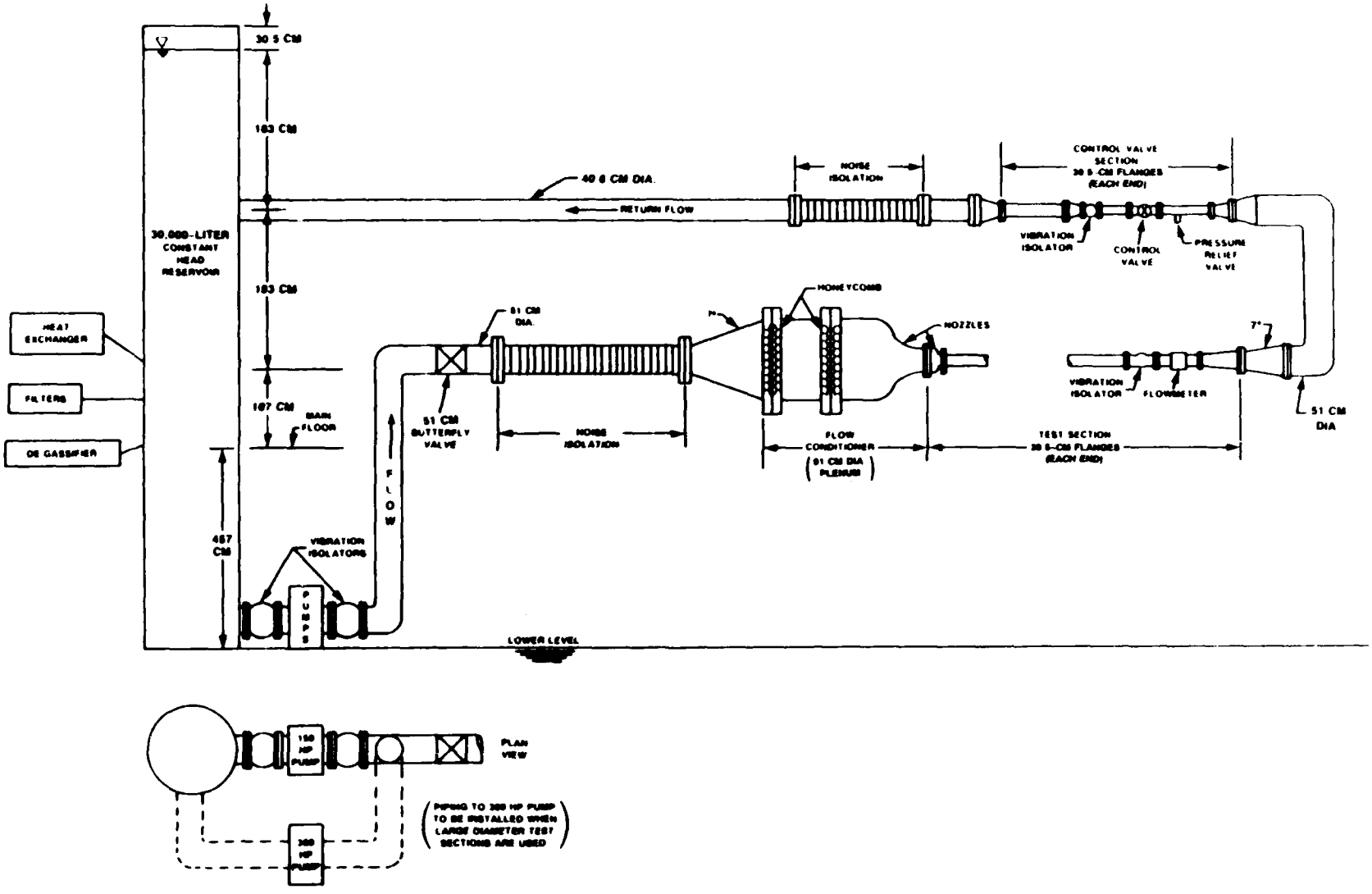

Figure 1. Flow Loop Facility Layout

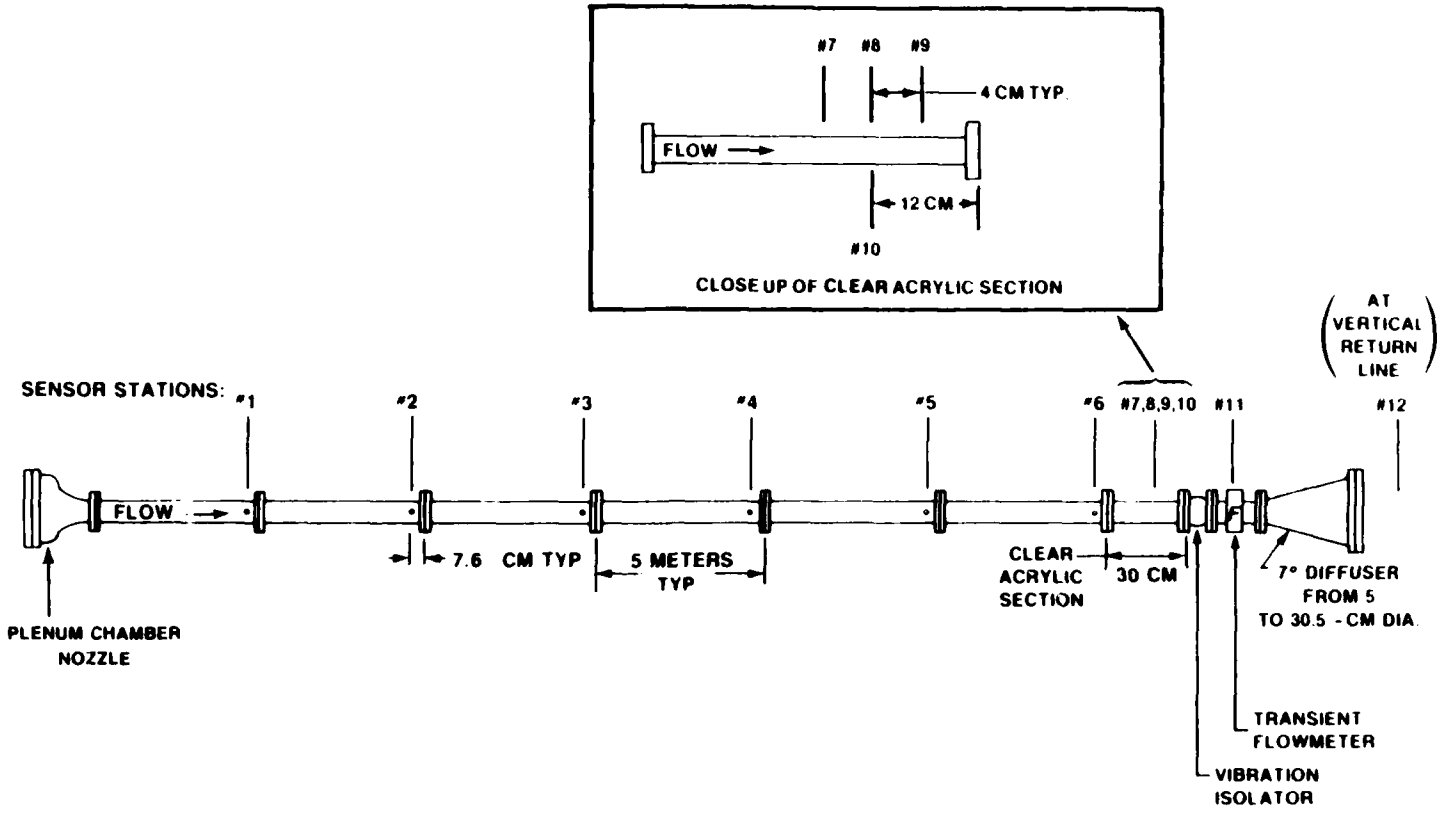

PHYSICAL SPECIFICATIONS
1 INSIDE DIAMETER - 5 ± .0025 CM
2 INSIDE SURFACE FINISH = 0.5 MICRONS
3 MATING AT FLANGES WITHIN 0.0025 CM
4 O-RING FACE SEAL AT FLANGES (NO HORIZONTAL GAP AT FLANGES)

STATION	INSTRUMENTATION
1 - 6	PRESSURE TAP/FLUSH PRESSURE SENSOR
1 - 10	SURFACE SHEAR STRESS SENSOR
8	LASER DOPPLER VELOCIMETER
11	TRANSIENT FLOWMETER
12	TEMPERATURE PROBE

Figure 2. 5-cm-Diameter Test Section

turbulence at transition (i.e., does the turbulence propagate from the wall toward the pipe centerline or vice-versa) and to better understand the characteristics of the transitional flow field.

For the second phase of the present project, a new 9-cm-diameter test section was built. As shown in figure 3, this circular test section consists of a 24.4-m-long section of PVC pipe followed by a 6.0-m-long cast acrylic section. The cast acrylic section was used mainly for LDV measurements while two hot-film wall shear stress sensors were placed in the PVC section at 12.2-m and 18.3-m from the entrance to the test section as shown in figure 3. For both the 5-cm-diameter and 9-cm-diameter test sections, care was taken to align adjacent pipe sections to minimize any step at the interface.

For the 9-cm-diameter test section, the control valve section of the flow loop facility also had to be modified. The original 7.6-cm Masoneilan anti-cavitation, anti-noise cage control valve was replaced with a larger 15.2-cm valve to accommodate the higher flow rates of the larger diameter test section. The new valve was a Jamesbury Corp. high-performance butterfly control valve. This valve provided good control over a wide range of accelerations and velocities.

For all test runs conducted under the present project, the control system was programmed to provide constant acceleration from rest, leveling off to a final steady mean velocity, which was sufficiently above the transition velocity so it would not affect transition itself. Mean flow accelerations ranged from 0.2 to 11.15 m/sec^2. Transition to turbulence was monitored by both the LDV, focused at the centerline of the test section, and the wall shear stress sensors. The time of transition was obvious in the abrupt change in the value of the measurements at transition.

The LDV system consisted of a 2-watt argon-ion laser with receiving optics configured in a forward-scattering mode. This mode was used to increase the valid data rate from the counter processor to a value between 10,000 and 50,000 samples/sec. Initial tests during the first project showed that the low data rates typical of backscattering techniques (approximately 400 samples/sec) were insufficient to follow the highly transient instantaneous velocities of these experiments.

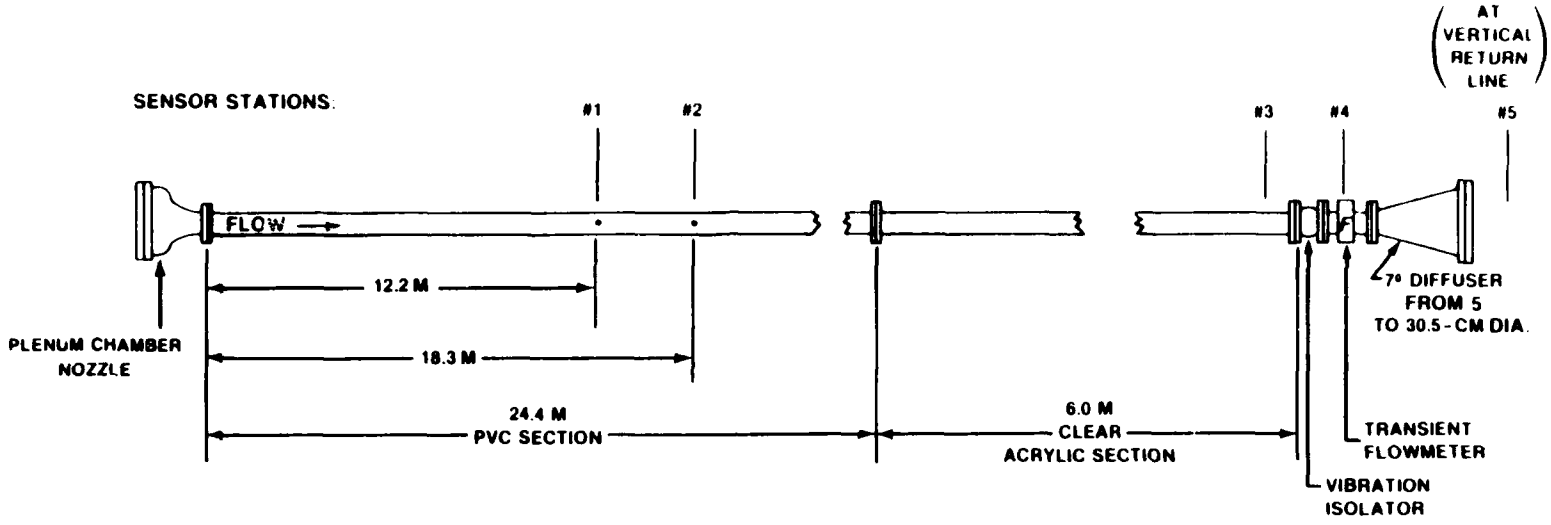

STATION	INSTRUMENTATION
1-2	SURFACE SHEAR STRESS SENSOR
3	LASER DOPPLER VELOCIMETER
4	TRANSIENT FLOWMETER
5	TEMPERATURE PROBE

Figure 3. 9-cm-Diameter Test Section

The LDV measuring volume was 0.93 mm long in the radial direction and 0.161 mm high. Since a large velocity range (more than 30 to 1) had to be accommodated with one setting of the LDV counter processor, an acousto-optic Bragg cell frequency shifter was used to effectively filter out the LDV signal's changing pedestal.

The hot-film wall shear stress sensors used were Thermal Systems Inc. (TSI) 1237-W (flush mounted). The hot-film anemometer used with the wall shear stress sensors was a TSI model #IFA 100. All data, including those from the transient flowmeter, wall shear stress sensors, and the LDV, were collected on a MASSCOMP MC500 digital data acquisition system at a sampling rate of 960 samples/sec. A specially designed interface was used between the MASSCOMP system and the LDV counter processor to permit periodic sampling of the LDV data. Details of the instrumentation and the test procedures are given in reference 1.

It should be noted that the Apple IIe computer, which was part of the control system and used to generate the transient command signal, also was used to trigger the start of the data acquisition by the MASSCOMP. The Apple computer then waited approximately 0.5 second after triggering data acquisition before starting the acceleration of the flow. All time history curves of the data that will be presented in this report will display this time delay.

COMPARISON WITH THEORY

The transition correlation parameters presented for the 9-cm-diameter test section data require the calculation of boundary layer thickness at the time of transition. As shown in reference 1 for the transition data from the 5-cm-diameter test section, the velocity profile in the pipe prior to transition agrees with the profile for startup of laminar pipe flow caused by a suddenly applied constant pressure gradient. A classic analytic solution for that case was given in reference 12. The solution for the unsteady velocity profile U(r,t) is given by:

$$\frac{U(r,t)}{U_{max}} = (1 - r^{*2}) - \sum_{n=1}^{\infty} \frac{8J_0(\lambda_n r^*)}{\lambda_n^3 J_1(\lambda_n)} e^{(-\lambda_n^2 t^*)} \qquad (1)$$

where $r^* = r/R$, $t^* = \upsilon t/R^2$, and λ_n are the zeros of the Bessel function J_0. The parameter $U_{max} = R^2(-dP/dx)/4\mu$ is the final maximum velocity corresponding to steady Poiseuille pipe flow. For t* approaching unity, U(r,t) approaches the Poiseuille flow; for $t^* < 0.05$, the centerline velocity increases linearly with time, simulating a constant acceleration startup.

The values of t* at transition varied from 0.000454 to 0.003654 for the experiments conducted on the 9-cm-diameter test section. These values are small enough for Szymanski's solution to be a valid approximation for the present experiments. Therefore, equation (1) will be used to predict the values of boundary layer thickness at transition which, in turn, will be used in the correlation parameter-boundary layer thickness Reynolds number.

RESULTS

In this section of the report, results are presented first for the data collected from the 5-cm-diameter test section and then for the data from the 9-cm-diameter test section. The 9-cm test section results are compared with the 5-cm test section results, which were presented in reference 1.

5-CM-DIAMETER TEST SECTION RESULTS

Prior to conducting detailed experiments aimed at investigating the physics of the transition process, an attempt was made to conduct accelerating flow tests from rest for the low acceleration range (<1.81 m/sec^2) not tested during the first project. Unfortunately, the control valve was inadequate for providing the very fine control required for these accelerations; a smooth, linear, velocity-versus-time curve was not possible. However, as will be discussed in the next section, the control system for the 9-cm-diameter test section was able to provide very constant accelerations of the mean flow down to 0.2 m/sec^2.

The main emphasis during testing on the 5-cm-diameter test section was to investigate, in detail, the physics of the flow field during the transition process. Specifically, insight into the generation and propagation of turbulence, as observed at the axial location where LDV measurements were made, was desired.

At the outset of the present project, a decision was made to limit the investigation to whatever information could be obtained by using only the measurement techniques developed and used during the previous project. Therefore, the clear acrylic test section was modified to include four hot-film wall shear stress sensors as described in the previous section. All time histories of the measurements on the 5-cm-diameter test section are plotted with 960 points per second of data.

A typical time history of the LDV pipe centerline velocity measurement for an acceleration of 1.86 m/sec^2 is shown in figure 4. The abrupt change

in magnitude followed by increased fluctuations about the mean curve are a clear indication of transition. Figure 5 shows the corresponding time history for shear stress sensors 6 through 10. Outputs for sensors 1 through 5 are not shown since they are similar to that of sensor 6, which was at the end of the last stainless steel section. As with the previous project's results reported in reference 1, transition occurred at approximately the same time for sensors 1 through 6 and the LDV.

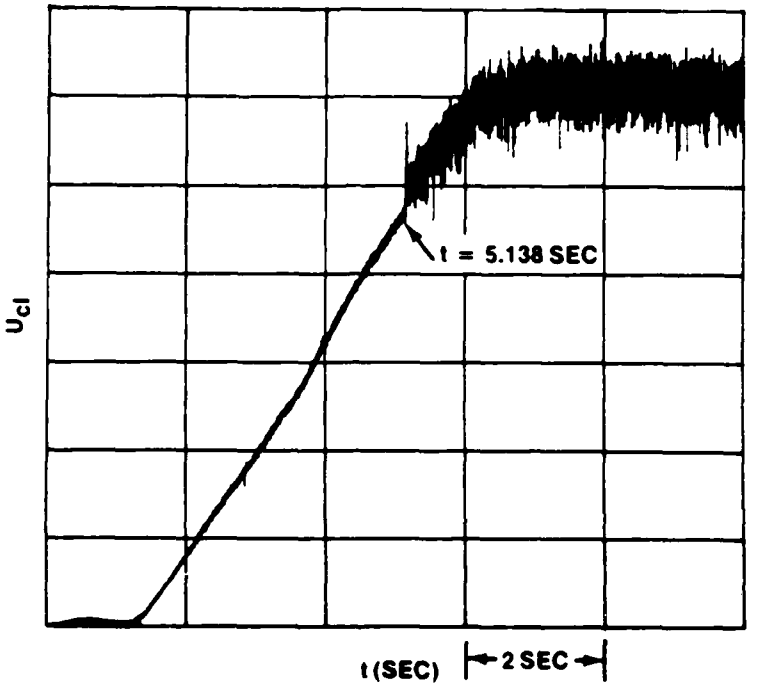

Figure 4. U_{cl} vs t; $\ddot{X} = 1.86$ m/sec^2 (5-cm Test Section)

The resulting shear sensor data for stations 7 through 10 are very unexpected. As shown, these four stations all experienced an instability that started at about the same time ($t \approx 4$ sec) but occurred approximately 1.1 seconds prior to transition to turbulence as observed at the LDV and the other shear stress stations. Station 10, unlike stations 7, 8, and 9, did fully transition abruptly at this early time without any region of instability. In figure 2, it is shown that station 10 was 180° from station 8 while stations 7, 8, and 9 were placed consecutively along the flow direction and spaced 4-cm apart. Throughout this 1.1-second duration of instability, the shear stress for stations 7, 8, and 9 experienced high-level fluctuations that were larger than the levels for fully turbulent flow.

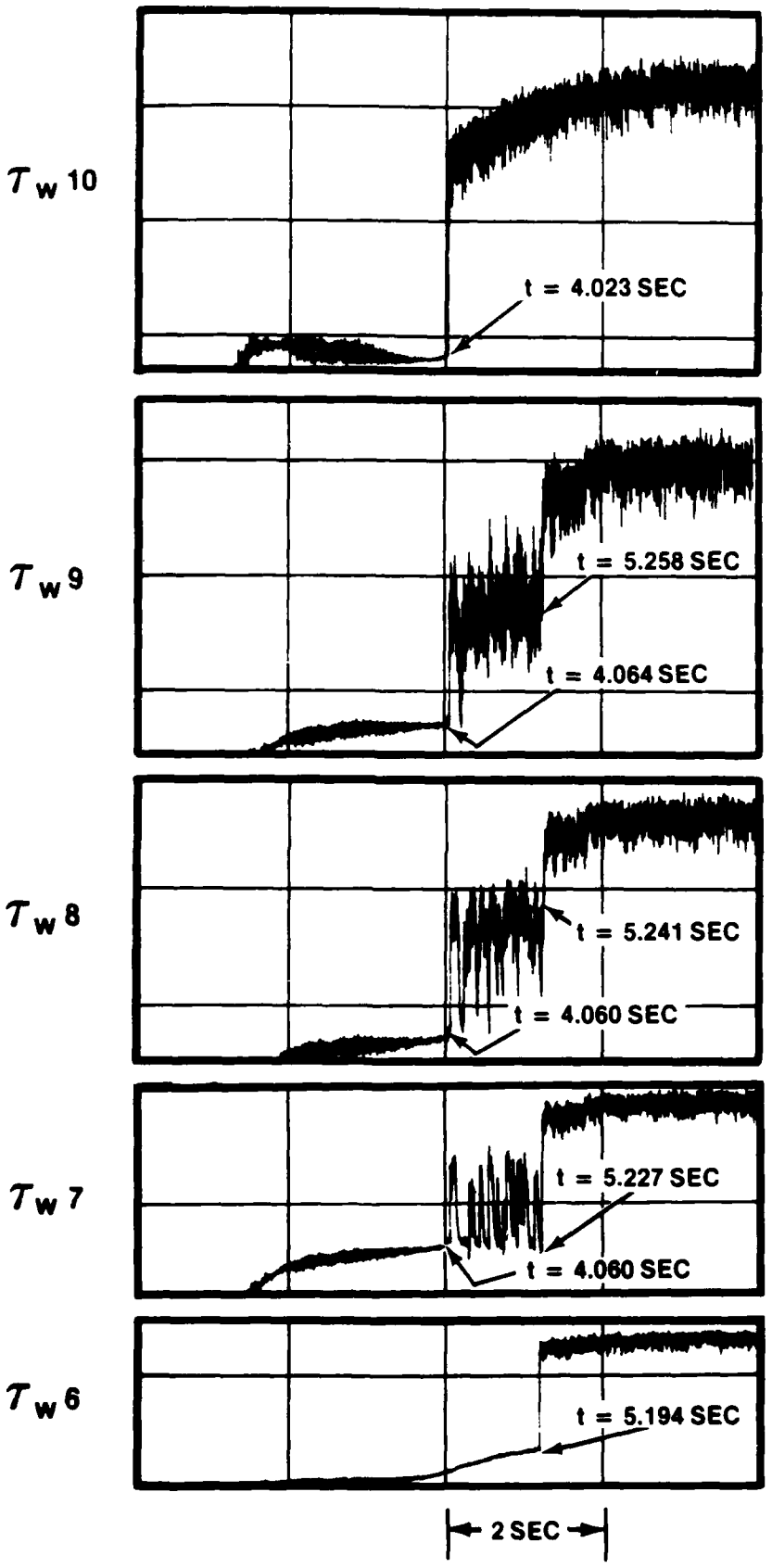

Figure 5. τ_w vs t; $\ddot{X}$ = 1.86 m/sec^2 (5-cm Test Section)

Figures 4 and 5 list the times at which each station became unstable and then fully turbulent. Station 10 became unstable (with abrupt transition) first. At 0.037 second later, stations 7 and 8 both became unstable at the same time (within the 0.001-second resolution of the data). Station 9 became unstable next, 0.004 second later. After another 1.074 seconds, a considerable delay, the LDV location transitioned to turbulence. This is interesting since this transition at the pipe centerline was 1.115 seconds later than that at station 10, which is at the same axial location. Station 6 then transitioned 0.056 second after the LDV. Note that station 6 is about 25.6 cm ahead of the LDV. Station 7 experienced full transition 0.033 second after station 6 followed by station 8 after another 0.014 second and then by station 9 after another 0.017 second.

From the previous measurements, it is impossible to explain the flow phenomena at transition except to say that there is very little indication of propagation effects in the downstream direction and there appears to be a substantial amount of local near-wall effects. The only propagation type effect can be seen in the transition at stations 7, 8, and 9. Other than that, there is no obvious connection between the various stations.

If there is indeed a propagation type effect from stations 7 through 9, then the convection velocity of the transition phenomenon can be estimated from the time information to be about 2.5 m/sec. Since the cross-sectional averaged velocity at the time of transition for these locations was 8.4 m/sec, the convection velocity was 30 percent of the cross-sectional averaged velocity.

The extended region of instability was never observed in any past experiments when the wall shear stress sensors were placed only in the stainless steel sections. It is interesting to note that, unlike transition to turbulence at stations 7, 8, and 9, the time of initial instability at these stations does not appear to have any axial propagation characteristics. This tends to reduce the likelihood that the reason for this instability phenomenon in the acrylic section is that the joint between the acrylic and the last steel section acts as a trip. Also, as noted previously, great care was taken to minimize any steps at joints.

Another fact indicating that transition in accelerating flows is not a propagation phenomenon is that the calculated convection velocity of transition from station 6 to 7 is inconsistent with that between stations 7 and 8 since it is 7.8 m/sec or three times higher than that between stations 7 and 8.

This instability phenomenon occurred consistently for repeat test runs at the same acceleration and similarly for higher accelerations up to about 3 m/sec^2. Beyond that acceleration, the region of instability was very short, if it existed at all.

Similar data to those just presented, but for an acceleration of 10.4 m/sec^2, follow. Figure 6 shows the time history of the LDV output for this case, while figure 7 presents the shear stress sensor output for stations 6 through 10. Again, transition occurred at approximately the same time for the LDV station and shear stress station 6. Only shear stress stations 8 and 9 experienced instability prior to full transition. As with the previous test runs, sensor station 10 transitioned earlier than all the other locations at a time of 0.67 second before the LDV and a substantial 0.18 second prior to station 9, the second wall location to become unstable. Station 8 then transitioned 0.014 second after station 9 first experienced some instability. Following another 0.096 second, station 7 transitioned. The LDV and station 6 transitioned 0.384 and 0.394 second, respectively, after station 7. Obviously, this "apparent" transition does not propagate in the flow direction. In addition, there was no apparent connection between stations 8, 10, and the LDV, which were all at the same axial location.

Since shear sensors 7 through 10 were fairly distant from the end of the acrylic section, it was difficult to ensure that the sensors were flush with the wall. A protruding sensor could locally affect the apparent transition. However, all the sensors tripped relatively early to turbulence, reducing the likelihood of protruding sensors.

The previous experiments reported in reference 1 showed that the velocity profile down to 0.13 cm from the wall transitioned virtually instantaneously from an almost uniform profile to the quasi-steady one. However, from the previously mentioned data for the two runs presented, it appears that there is

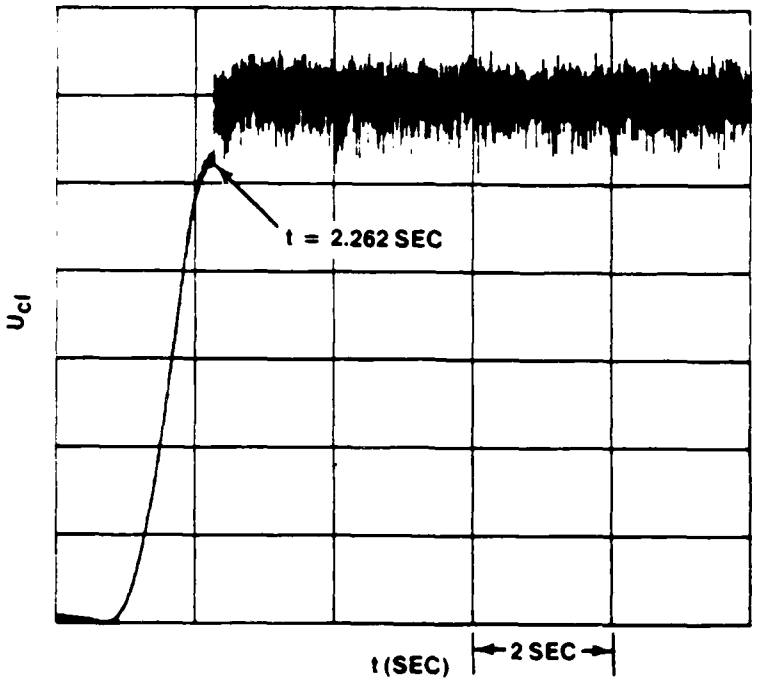

Figure 6. U_{cl} vs t; $\ddot{X}$ = 10.4 m/sec^2 (5-cm Test Section)

a substantial amount of near-wall phenomena occurring locally along the test section. Since the boundary layer thickness at transition ranged from δ/R of 0.045 to 0.182, it is possible that, at some axial locations, the near-wall flow acted as flat plate flow; any instabilities remained within the boundary layer and did not affect the core flow. Then at a later time, full transition occurred virtually globally throughout the test section and the complete profile became turbulent.

The flow field in the vicinity of the LDV is obviously very complex. For a complete understanding of the flow field, flow visualization is required. Instantaneous two-dimensional flow visualization of a thin slice of the flow field along the axial direction and extending from stations 7 to 9 and across the diameter would be ideal. Potential techniques for these measurements are now being developed by others and should be investigated for any future work in this area.

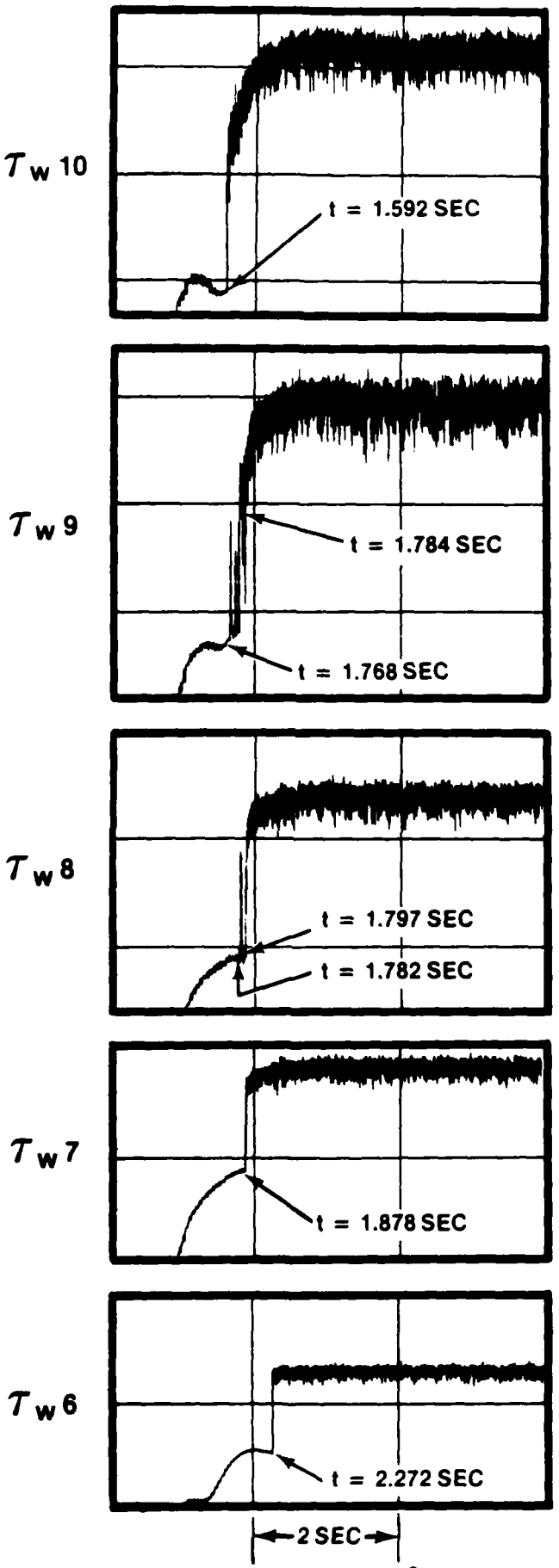

Figure 7. τ_w vs t; $\ddot{X}$ = 10.4 m/sec^2 (5-cm Test Section)

9-CM-DIAMETER TEST SECTION RESULTS

A total of 32 test runs were conducted on the 9-cm-diameter test section. Each acceleration run was started from rest in an attempt to determine the time and conditions of transition to turbulence. All figures in this section, which show time histories of the measurements, are plotted at 120 points/second of data. Note that in these time histories the time $t = 0.0$ second is at the start of data acquisition and that the actual acceleration begins approximately 0.5 second later.

Figures 8 through 10 show the resulting linear cross-sectional averaged velocity versus time for three different test runs at accelerations of 0.2, 6.3, and 11.15 m/sec^2, respectively. These runs cover the range of accelerations tested, which varied from 0.2 to 11.15 m/sec^2. The high linearity of these curves verifies that constant acceleration was indeed obtained. On each of the figures, the time at which transition occurred (as evidence by the wall shear stress sensors and the LDV) is noted. It is obvious that transition to turbulence did not affect the acceleration.

It was fortunate that the flow loop facility, as configured for the 9-cm-diameter test section, could provide substantially lower accelerations than was possible with the 5-cm section. As shown in the following discussion of results, the new data add substantially to the data base from the 5-cm tests.

Figures 11 through 13 are the time histories of the output from the two wall shear stress sensors for the three runs of figures 8 through 10 (i.e, accelerations of 0.2, 6.3, and 11.15 m/sec^2, respectively). Since only the time of transition was of interest and not the absolute magnitude of the wall shear stress, the sensors were not calibrated. The time of transition is clear where the sensor output increases almost instantaneously.

For each of the 32 runs, the time of transition was essentially global, that is, transition occurred abruptly and at virtually the same instance in time as indicated by the various measurements. Transition times generally differed by less than 3 percent with a few runs at a maximum of 10 percent when based on the time from the start of the acceleration.

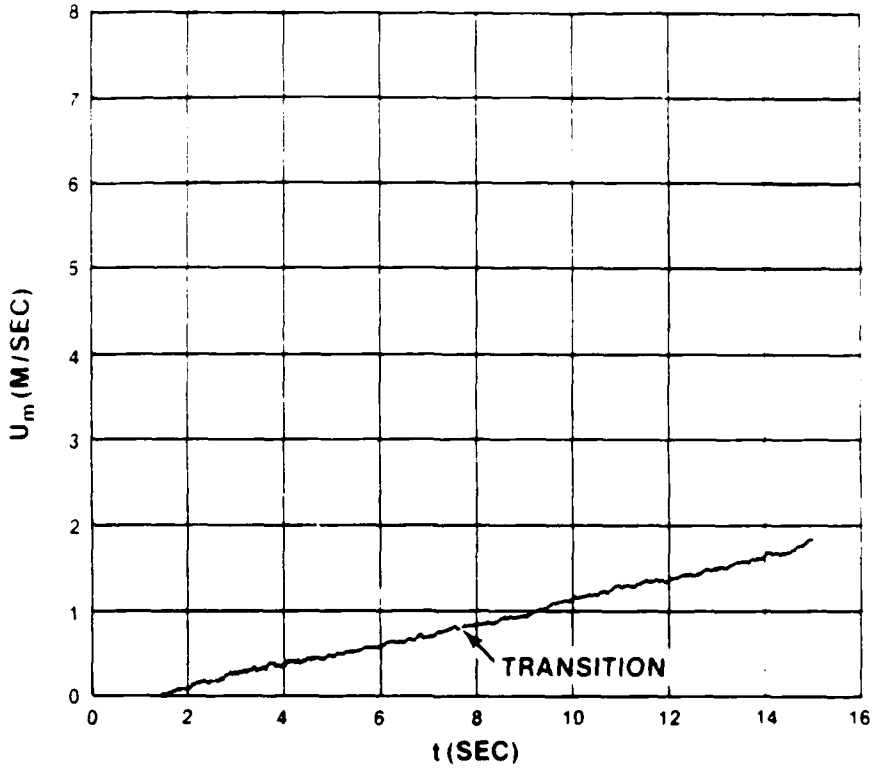

Figure 8. U_m vs t; $\ddot{X}$ = 0.2 m/sec^2

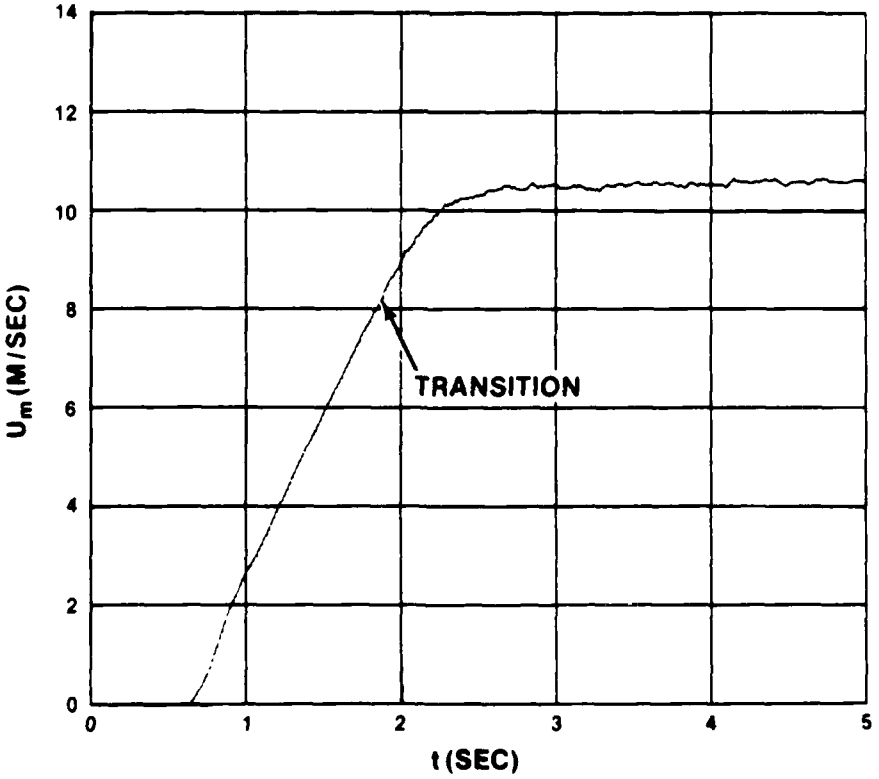

Figure 9. U_m vs t; $\ddot{X}$ = 6.3 m/sec^2

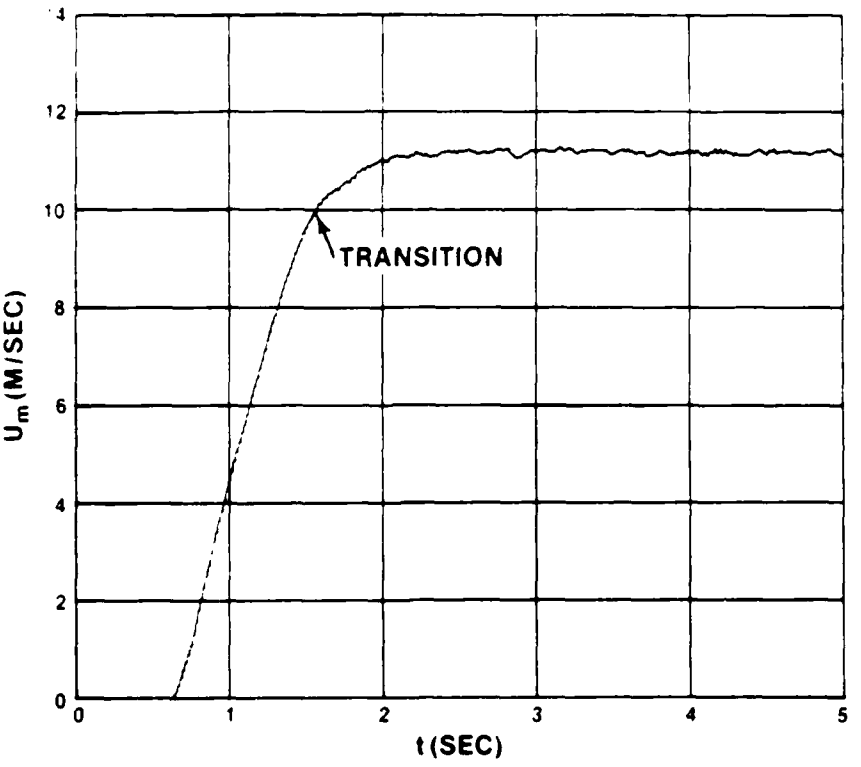

Figure 10. U_m vs t; $\ddot{X}$ = 11.15 m/sec^2

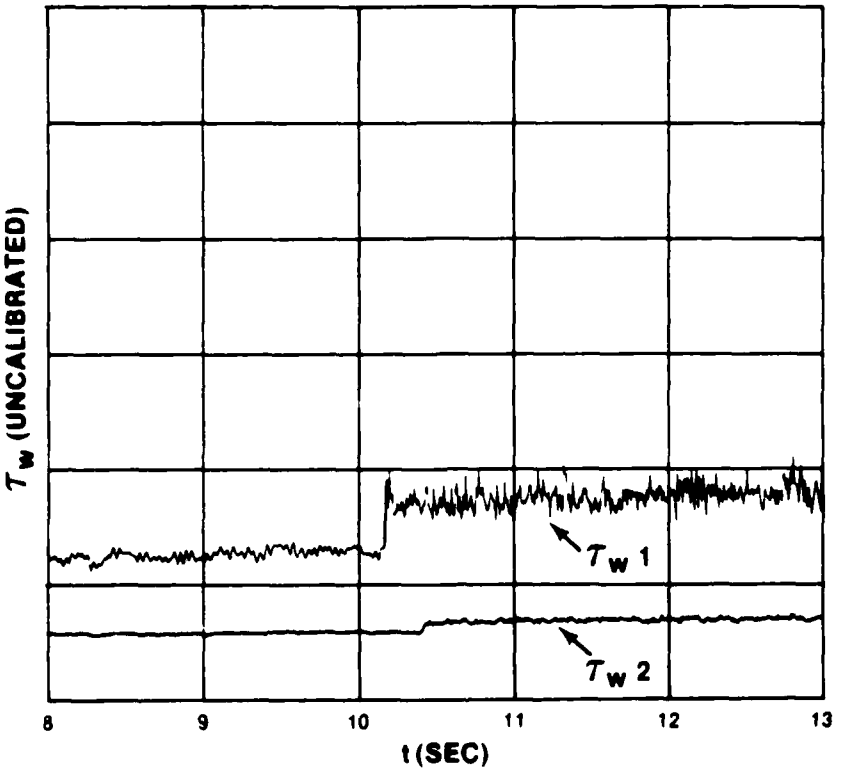

Figure 11. τ_w vs t; $\ddot{X}$ = 0.2 m/sec^2

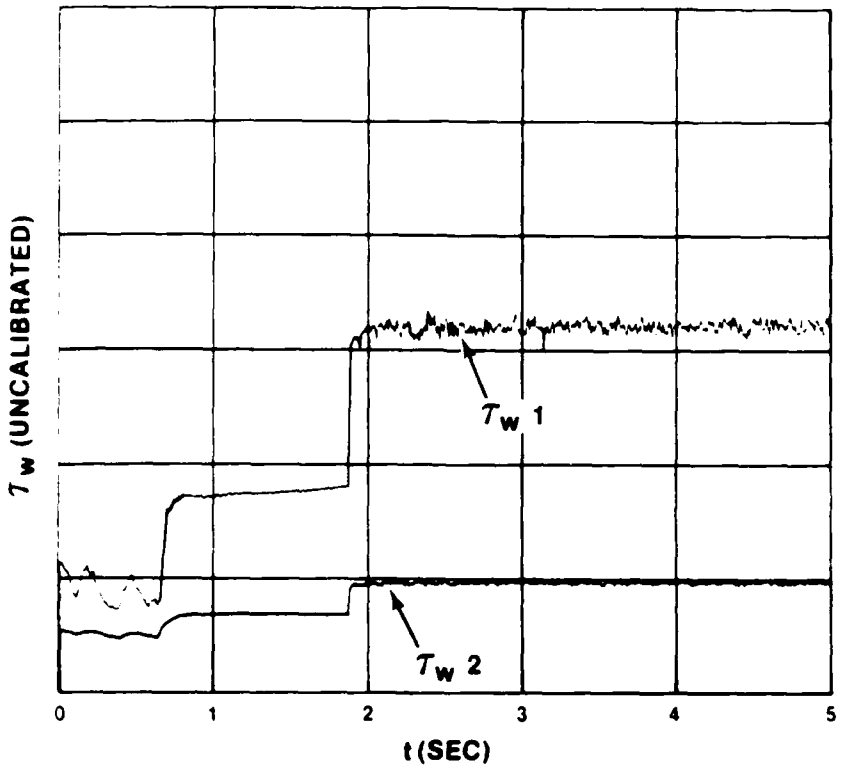

Figure 12. τ_w vs t; $\ddot{X}$ = 6.3 m/sec^2

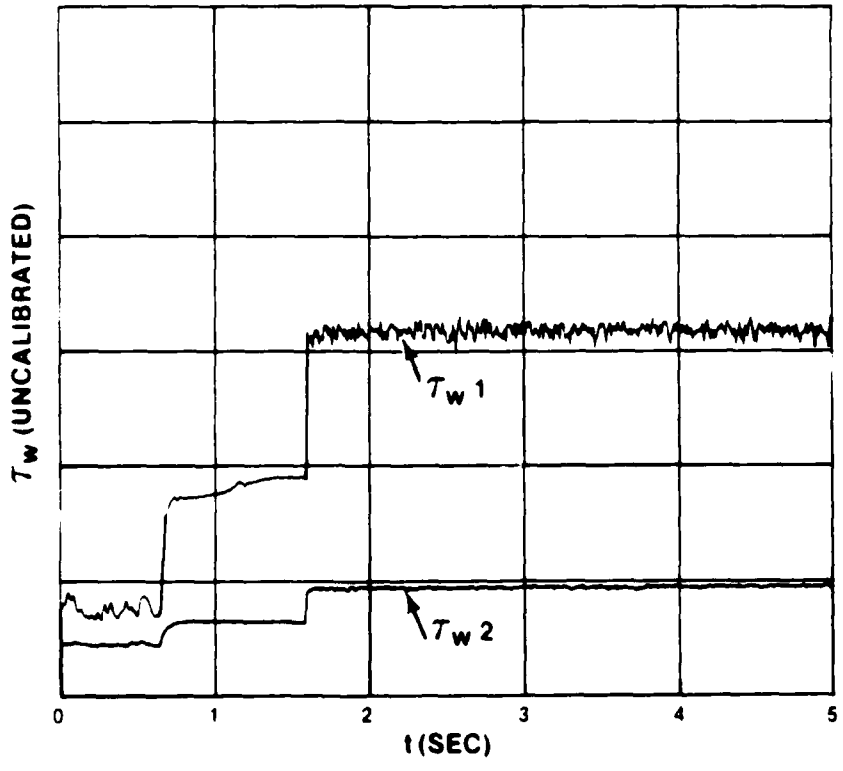

Figure 13. τ_w vs t; $\ddot{X}$ = 11.15 m/sec^2

Table 1 lists the correlation parameters calculated for the 32 runs. Test runs are presented in order of increasing acceleration and include U_f = final steady state velocity, T = temperature, ν = kinematic viscosity, $U_{m,tr}$ = cross-sectional mean velocity at transition, $t_{eff,tr}$ = time of transition from the start of the transient (not the start of data acquisition), and t^*_{tr} = nondimensional time at transition based on $t_{eff,tr}$. Note that $t_{eff,tr}$ is the effective time of transition as calculated by $t_{eff,tr} = U_{m,tr}/\ddot{X}$ to account for the delay between the start of data acquisition and the transient.

As in reference 1, the transition correlation parameters are $Re_{D,tr}$ = pipe Reynolds number, $K_{a,tr}$ = local acceleration parameter at transition, and $Re_{\delta,tr}$ = boundary layer thickness Reynolds number at transition, where

$$Re_{D,tr} = D * U_{m,tr}/\nu, \tag{2}$$

$$Re_{\delta,tr} = \delta_{tr} * U_{m,tr}/\nu, \tag{3}$$

$$K_a = (\nu/U^3_{m,tr}) * (dU_m/dt). \tag{4}$$

The first correlation of the transition data is shown in figure 14 where acceleration is plotted against $Re_{D,tr}$. The curve for the 9-cm data is shown along with that for the 5-cm data. The data for each individual test section do follow a trend of increasing $Re_{D,tr}$ with increasing acceleration, but the data for each do not agree with each other. These parameters, therefore, are obviously inadequate as a transition correlation, but the data show that all of the values of $Re_{D,tr}$ are extremely high (up to $Re_{D,tr}$ of 1.11×10^6) relative to the steady-state transition value of approximately 2000 for pipe flow.

Figure 15 shows $Re_{D,tr}$ vs t^*_{tr}. It can be seen that neither of the two parameters are constant at the transition point of an accelerating flow. However, as stated in reference 1 for the 5-cm-diameter test section, these two parameters do seem to correlate with each other. At the lower $Re_{D,tr}$ values, the correlation between the 5-cm and 9-cm data is reasonably good; the

Table 1. Transition Parameters; 9-cm-Diameter Test Section

Run No.	$\ddot{X}$ (m/sec^2)	U_f (m/sec)	T (°C)	υ (m^2/sec)($x10^7$)	U_m (m/sec)	K_a ($x10^{-8}$)	Re_{D_5} ($x10^5$)	t_{eff} (sec)	$t^* = \upsilon t/R^2$	δ/R	Re_δ
1	0.20	2.4	24.9	9.00	1.33	7.65	1.34	6.65	0.002911	0.163	10921
2	0.20	2.4	23.8	9.22	1.33	7.84	1.31	6.65	0.002983	0.165	10791
3	0.24	3.6	23.6	9.27	1.93	3.09	1.89	8.04	0.003626	0.171	17085
4	0.24	3.6	23.7	9.25	1.95	2.99	1.91	8.12	0.003654	0.182	17395
5	0.61	7.6	23.7	9.25	2.88	2.36	2.82	4.72	0.002124	0.143	20186
6	0.61	7.6	23.7	9.25	2.83	2.49	2.77	4.64	0.002088	0.142	19696
7	0.87	7.6	23.7	9.25	3.47	1.93	3.40	3.99	0.001795	0.129	21940
8	0.87	7.6	23.7	9.25	3.46	1.94	3.39	3.98	0.001791	0.129	21877
9	1.25	10.7	23.7	9.25	4.06	1.73	3.98	3.25	0.001462	0.112	22287
10	1.25	10.7	23.7	9.25	4.02	1.78	3.94	3.20	0.001440	0.111	21871
11	1.85	10.7	23.6	9.27	3.93	2.82	3.84	2.12	0.000956	0.082	15761
12	1.85	10.7	23.6	9.27	4.31	2.14	4.22	2.33	0.001051	0.088	18550
13	3.70	10.7	23.5	9.29	6.90	1.05	6.73	1.86	0.000841	0.074	24919
14	3.70	10.7	23.5	9.29	6.91	1.04	6.74	1.87	0.000845	0.074	24955
15	4.41	10.7	23.7	9.25	7.54	0.95	7.39	1.71	0.000769	0.069	25500
16	4.50	10.7	23.6	9.27	7.87	0.86	7.70	1.75	0.000789	0.070	26943
17	5.50	10.7	23.7	9.24	8.66	0.78	8.50	1.57	0.000706	0.065	27620
18	5.60	10.7	23.3	9.32	7.99	1.02	7.77	1.43	0.000648	0.060	23321
19	5.65	10.7	23.3	9.32	8.66	0.81	8.43	1.53	0.000694	0.064	26961
20	6.30	10.7	23.7	9.25	9.16	0.76	8.98	1.45	0.000652	0.061	27387
21	6.30	10.7	23.7	9.25	9.25	0.74	9.07	1.47	0.000661	0.061	27656
22	7.10	10.7	23.6	9.27	9.90	0.68	9.68	1.39	0.000627	0.059	28567
23	7.20	10.7	23.7	9.25	9.85	0.70	9.66	1.37	0.000616	0.058	28000
24	8.10	10.7	23.6	9.27	10.14	0.72	9.92	1.25	0.000564	0.054	26780
25	8.10	10.7	23.6	9.27	10.31	0.68	10.01	1.27	0.000573	0.055	27733
26	8.55	10.7	23.4	9.30	10.32	0.72	10.06	1.21	0.000547	0.053	26664
27	8.75	10.7	23.5	9.29	10.59	0.68	10.34	1.21	0.000547	0.053	27391
28	9.45	10.7	23.6	9.27	10.72	0.71	10.49	1.13	0.000510	0.050	26215
29	9.60	10.7	23.5	9.28	10.81	0.70	10.56	1.13	0.000510	0.050	26406
30	10.10	11.2	23.5	9.28	11.15	0.68	10.89	1.10	0.000497	0.049	26692
31	11.15	11.2	23.6	9.27	11.39	0.70	11.14	1.02	0.000460	0.046	25625
32	11.15	11.2	23.7	9.25	11.29	0.72	11.07	1.01	0.000454	0.045	24901

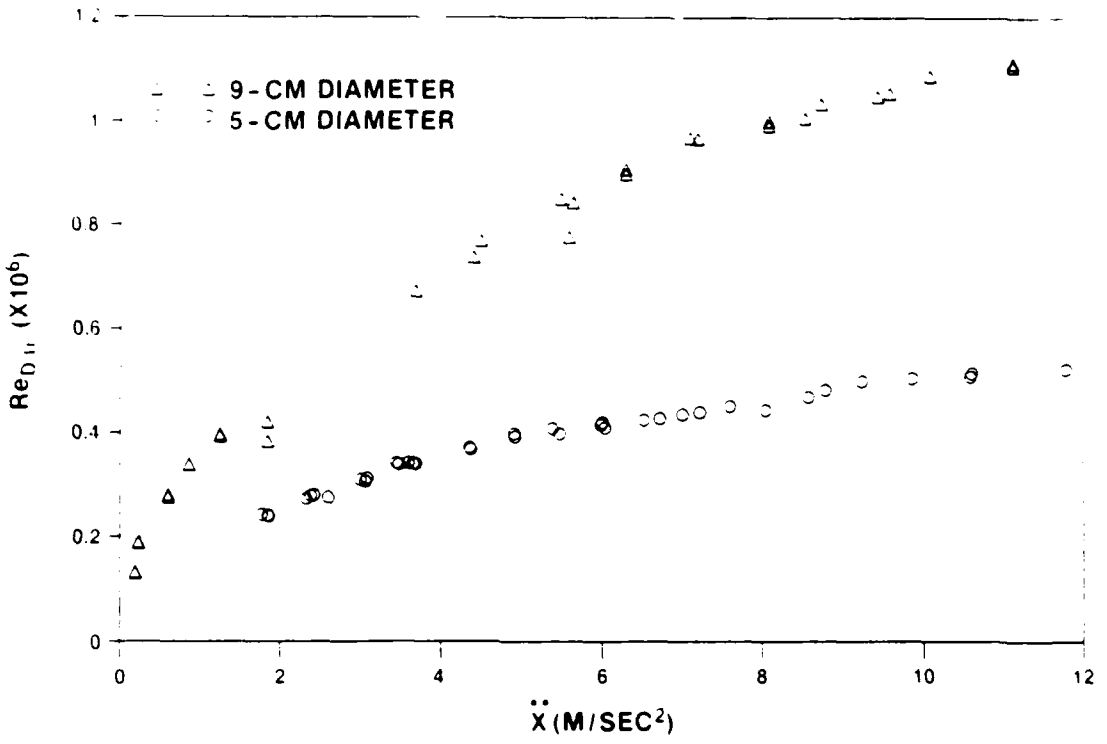

Figure 14. Re_D vs $\ddot{X}$ at Transition

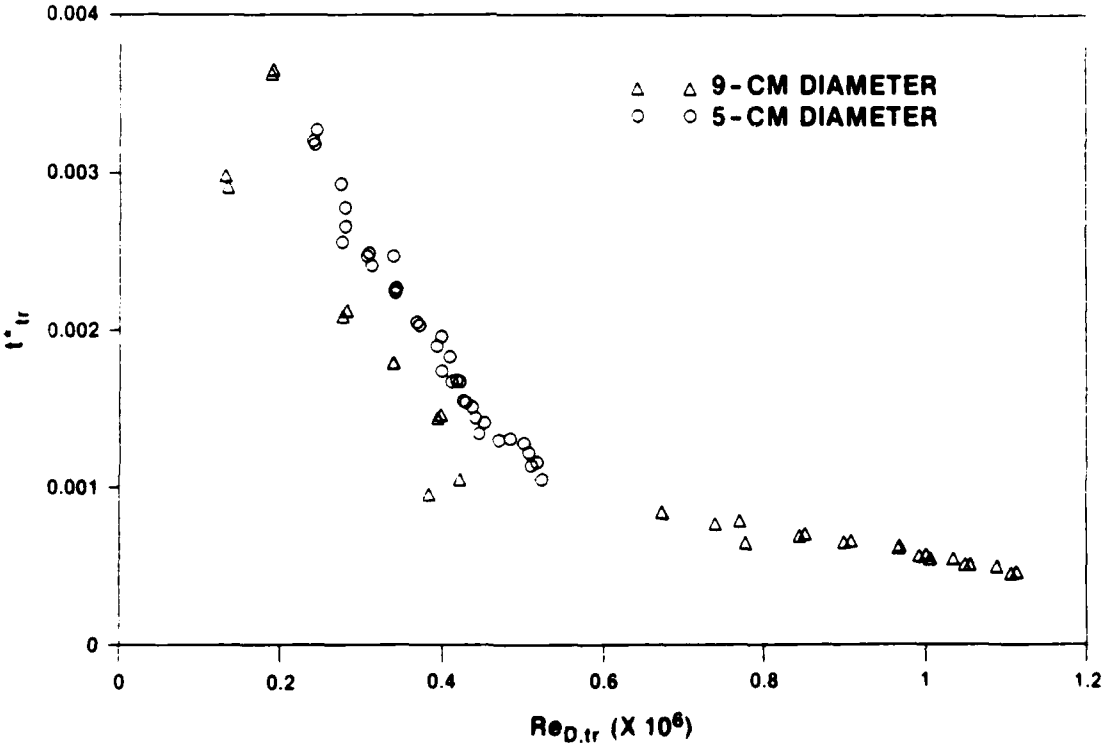

Figure 15. t* vs Re_D at Transition

9-cm section data being only slightly lower but following the same trend as the 5-cm data. For the higher $Re_{D,tr}$ ($Re_{D,tr} > 6 \times 10^5$), the values of $Re_{D,tr}$ approach a constant value of approximately 1.1×10^6. Again, even though the parameters do seem to correlate well between test sections, $Re_{D,tr}$ does not appear to be an adequate correlation parameter since it does not include realistic size or length scale information. That is, as shown in reference 1, the boundary layer at the wall at the time of transition is very small and does not extend to the pipe centerline, thereby making the pipe Reynolds number questionable.

In reference 1, an attempt was made to develop a correlation parameter for local acceleration, which was the analog of the convective acceleration parameter, $K = (\nu/U^2)(dU/dx)$, which is commonly used for relaminarization. The local acceleration parameter that was developed was K_a, as given by equation (3). A detailed discussion of the parameter K is given in reference 1.

The curve of K_a vs $Re_{D,tr}$ is plotted in figure 16. For the lower $Re_{D,tr}$ where the 9-cm and 5-cm data overlap, good agreement for the two cases is evident. For the larger $Re_{D,tr}$, the 9-cm data follow the same trend as observed for the 5-cm data in that the value of K_a asymptotically approaches a lower value as $Re_{D,tr}$ increases. For the 9-cm data, the value is approximately 0.7×10^{-8}. The data for $K_a < 4.0 \times 10^{-8}$ are replotted in figure 17 to give a better indication of the trend. It is obvious that this curve appears to be a reasonable choice for correlating transition data; however, it does not appear that the lower value of K_a has as yet been reached.

The last attempt described in reference 1 to arrive at a reasonable correlation was to plot $Re_{\delta,tr}$ versus acceleration. This correlation includes realistic length scale information in $Re_{\delta,tr}$. Figure 18 is a plot of these variables for both the previous 5-cm data and the present 9-cm data. For the range of accelerations, 1.8 to 11.8 m/sec^2 (where data were obtained on both test sections), excellent correlation between the two sets of data are evident.

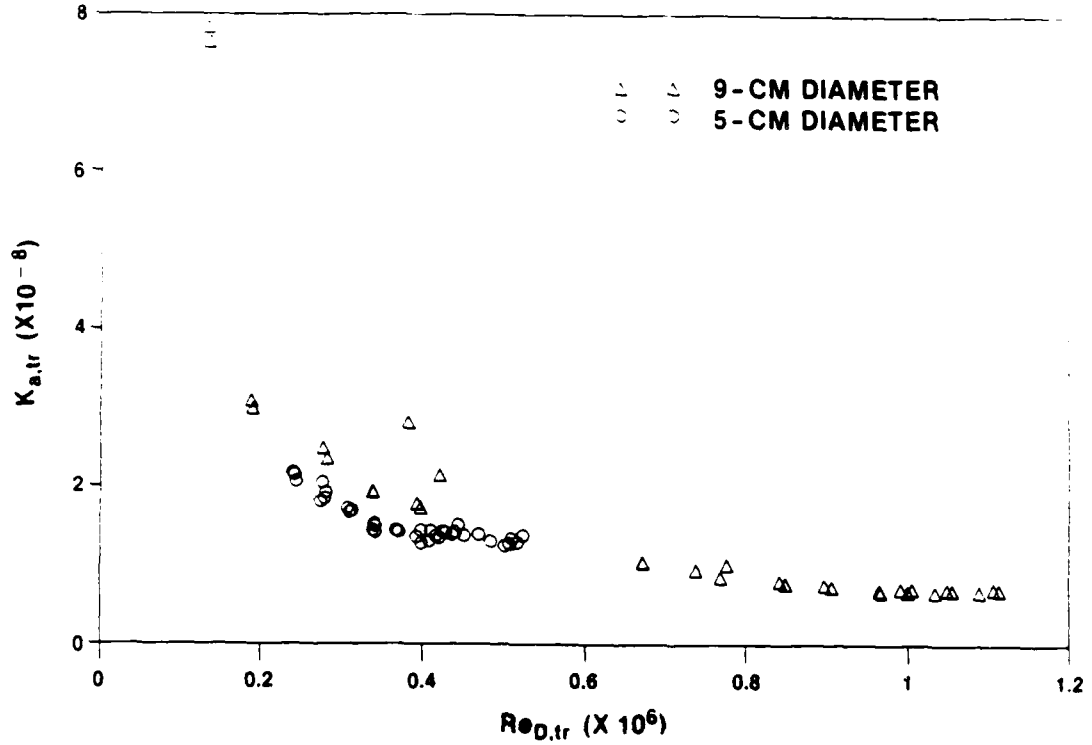

Figure 16. K_a vs Re_D at Transition

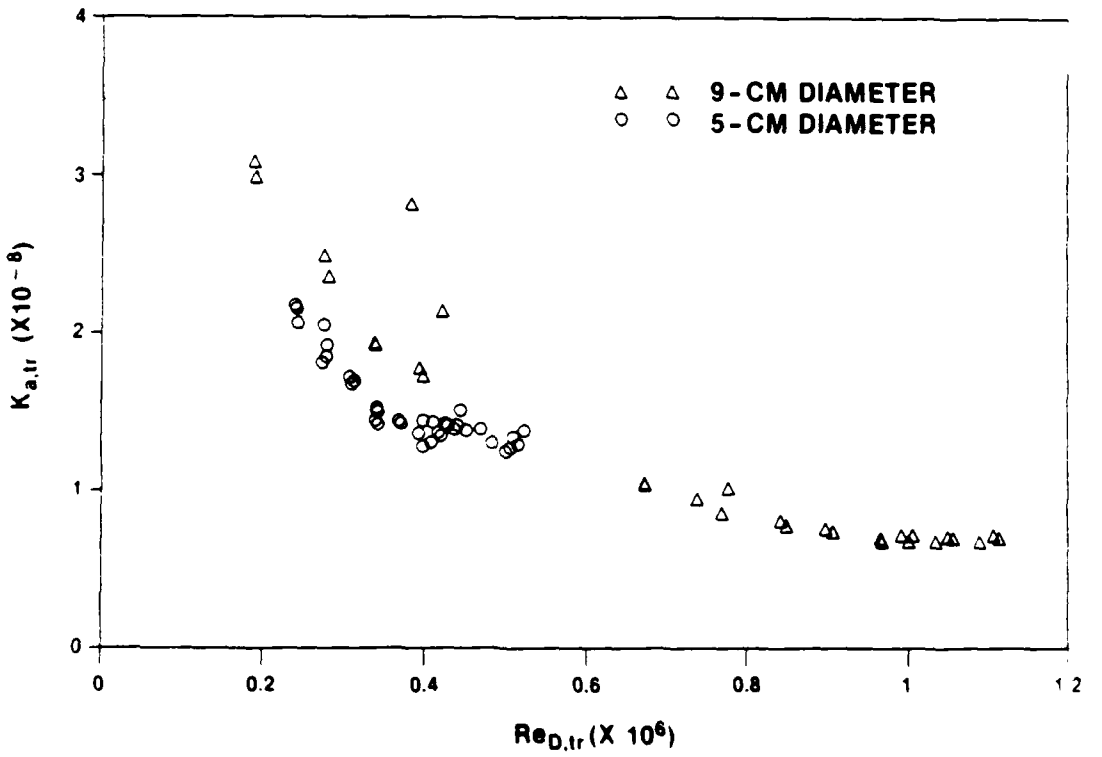

Figure 17. K_a vs Re_D at Transition

For the acceleration range above 3 m/sec^2, the value of $Re_{\delta,tr}$ is, as desired, approximately constant. The mean value of $Re_{\delta,tr}$ for the 5-cm data is 24984 $\pm$ 7.8 percent, while for the 9-cm data the value is 26511 $\pm$ 9.5 percent. For the 50 test runs above 3 m/sec^2 from both the 5-cm and 9-cm test section data, the mean value of $Re_{\delta,tr}$ is 25,595 $\pm$ 10.4 percent. The scatter about the mean values were calculated at the 95-percent (two standard deviations) confidence level.

For the lower accelerations, 0.2 to 1.8 m/sec^2, obtained on the 9-cm-diameter test section, the value of $Re_{\delta,tr}$ decreases with decreasing acceleration. In fact, the shape of the mean curve for this range is very similar to that predicted through an extrapolation in reference 3. This trend with decreasing acceleration is seen to asymptotically approach the steady state (zero acceleration) transition Re_δ value of approximately 2000 for flat plate flow. It is interesting to note that for the lowest acceleration tested, 0.2 m/sec^2, which is a mere 1/49 of the acceleration due to gravity, the value of Re_δ is approximately 10,500, still five times higher than the zero acceleration value.

This trend of decreasing Re_δ is substantiated by the single experiment of van de Sande et al. (reference 7). They report transition during the acceleration phase of startup flow in a pipe. In their experiment, they used a quick-opening valve and a constant-head tank to generate accelerating flow in a 5-cm-diameter water pipe. Their experiments were limited to very low accelerations. For one of their runs, transition occurred at t + 4.2 sec, corresponding to a mean velocity of 1.15 m/sec and a Reynolds number $Re_{D,tr}$ + 57500. From figure 8 in reference 7, one can estimate that the very low acceleration at the transition point was about 0.1 m/sec^2. The estimated value of Re_δ = 8600 is given in figure 18 and is shown to follow the trend of the present 9-cm data.

An interesting observation was made for three of the test runs conducted on the 9-cm-diameter test section. As shown in figures 19 and 20 for the accelerations of 1.25 and 7.1 m/sec^2, respectively, the flow at wall shear stress sensor number 2 tripped to turbulence earlier than expected but then

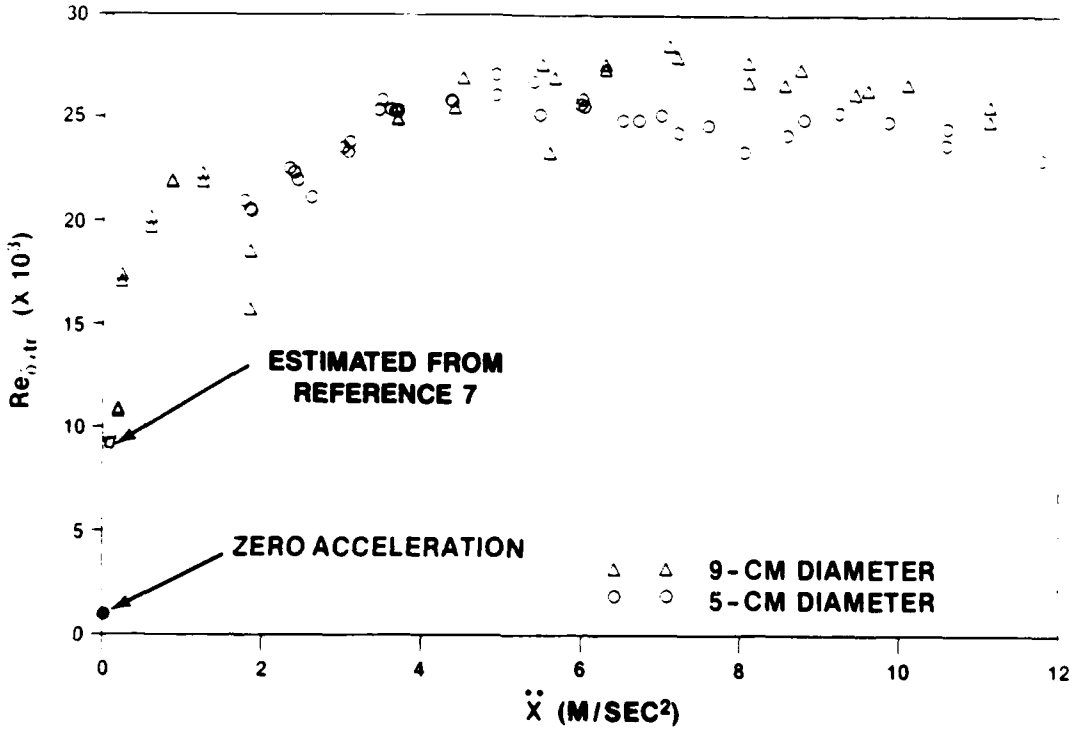

Figure 18. Re_δ vs $\ddot{X}$ at Transition

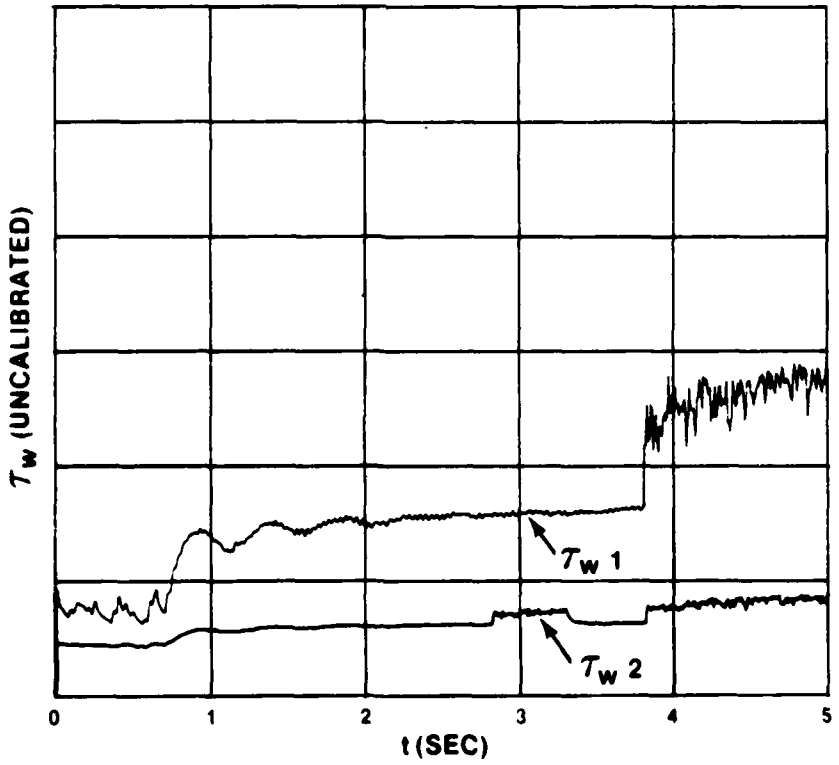

Figure 19. τ_w vs t; $\ddot{X}$ = 1.25 m/sec^2

relaminarized prior to the final transition at the expected time coincident with transition at sensor number 1. In figure 21, for an acceleration of 5.65 m/sec^2, a similar phenomenon occurred but, this time, sensor number 1 exhibited the premature transition.

Some local instability is the likely cause for the initial transition. However, from the limited wall shear stress measurements, it can only be assumed that the reversion back to a laminar type signal is due to the passing of some sort of turbulent puff, which was confined to a relatively short length of the test section. By using the known mean velocity at the beginning and end of the first turbulent region, the puff's length was estimated to be 1.3 m for the 1.25 m/sec^2 acceleration of figure 19, 2.0 m for the 7.10 m/sec^2 acceleration of figure 20, and 1.2 m for the 5.65 m/sec^2 acceleration of figure 21.

It is unlikely that relaminarization due to the stabilizing effect of the acceleration occurs. Some justification for that statement can be obtained from previous experiments reported in reference 1. There, relaminarization was not observed for an initially low velocity turbulent flow undergoing constant acceleration. This interesting phenomenon would be a good topic for further investigation.

It should be noted that for the three runs that exhibited the two transition points, the t*'s presented earlier were calculated using the time of the final transition point.

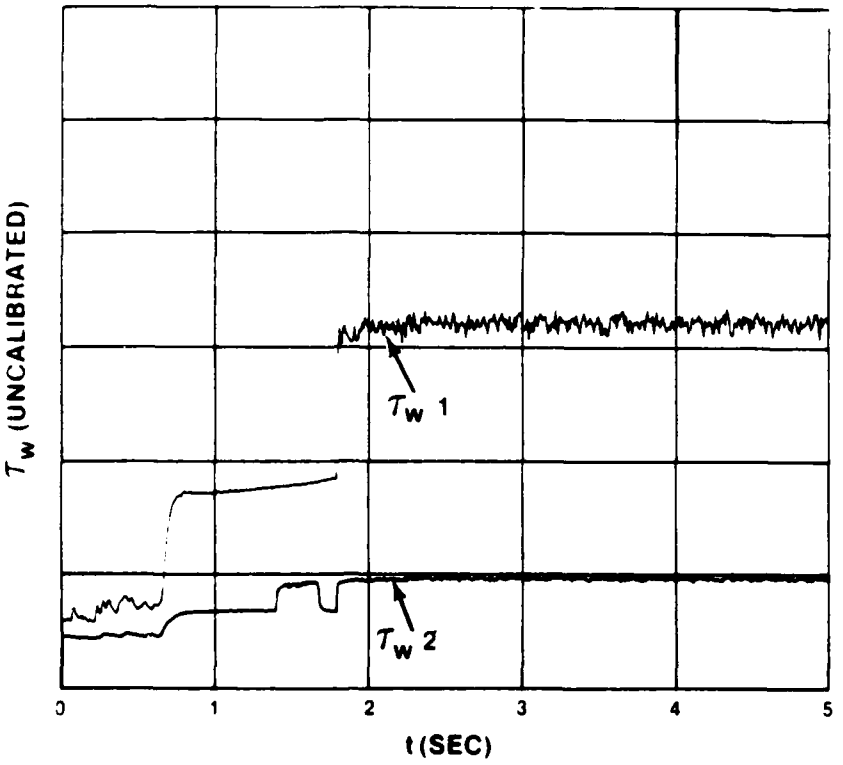

Figure 20. τ_w vs t; $\ddot{X}$ = 7.1 m/sec^2

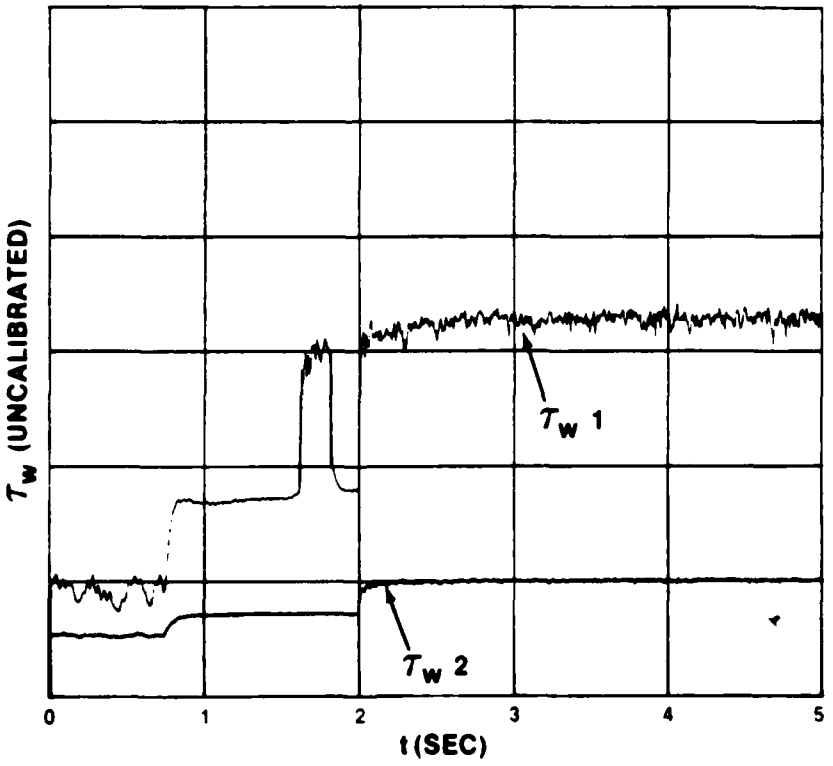

Figure 21. τ_w vs t; $\ddot{X}$ = 5.65 m/sec^2

CONCLUSIONS

A unique series of experiments was conducted on the laminar-to-turbulent transition in constant-acceleration pipe flow. The major conclusions resulting from this study are:

1. The main effect of mean acceleration on the flow field is to stabilize the flow to such a great extent that transition to turbulence is considerably delayed.

2. Pipe Reynolds numbers at the point of transition in accelerating flows have been observed to be as high 1.1×10^6, substantially higher than the steady-state, zero-acceleration value of approximately 2×10^3.

3. The correlation parameters for predicting transition in constant-acceleration pipe flow, namely, K_a and Re_δ, have been validated as being reasonable and accurate.

4. The details of the flow field at the time of transition are very complex. It appears that some local effects lead to local instabilities and possibly transition that are confined to the near-wall region.

5. A comprehensive understanding of the flow field is impossible without a global investigative technique such as laser-speckle velocimetry flow visualization.

REFERENCES

1. P.J. Lefebvre, "Characterization of Accelerating Pipe Flow," Ph.D. Dissertation, University of Rhode Island, Kingston, RI, 1987.

2. P.J. Lefebvre, "Design and Evaluation of NUSC's Flow Loop Facility," NUSC Technical Document 6512, Naval Underwater Systems Center, Newport, RI, May 1986 (UNCLASSIFIED).

3. E.B. Denison, "Pulsating Laminar Flow Measurements with a Directionally Sensitive Laser Velocimeter," Ph.D. Thesis, Purdue University, West Lafayette, IN, 1970.

4. T. Mizushina, T. Maruyama, and H. Hirasawa, "Structure of the Turbulence in Pulsating Pipe Flows," Journal of Chemical Engineering of Japan, vol 8, no. 3, pp 210-216, 1975.

5. B.R. Ramaprian and S.W. Tu, "Study of Periodic Turbulent Pipe Flow," IIHR Report 238, Iowa Institute of Hydraulic Research, 1982.

6. R. Carsten and J.E. Roller, "Boundary-Shear Stress in Unsteady Turbulent Pipe Flow," Journal of the Hydraulics Division, ASCE, vol 2, pp 67-81, February 1959.

7. E. van de Sande, A.P. Belde, B.J.G. Hamer, and W. Hiemstra, "Velocity Profiles in Accelerating Pipe Flows Started from Rest," Third International Conference on Pressure Surges, Canterbury, England, March 1980.

8. S.V. Denison, "The Friction Coefficient in Nonstationary Flows," Journal of Engineering Physics, vol 18, pt 1, pp 88-92, January 1970.

9. K. Kataoka, T. Kawabata, and K. Miki, "The Start-Up Response of Pipe Flow to a Step Change in Flow Rate," Journal of Chemical Engineering of Japan," vol 8, no. 4, pp 266-271, 1975.

10. T. Maruyama, T. Kuribayashi, and T. Mizushina, "The Structure of Turbulence in Transient Pipe Flows," Journal of Chemical Engineering of Japan, vol 9, no. 6, pp 431-439, 1975.

11. P.J. Lefebvre and W.W. Durgin, "A Transient Electromagnetic Flowmeter, "Measuring and Metering of Unsteady Flows, ASME-FED, vol 40, December 1986.

12. P. Szymanski, "Some Exact Solutions of the Hydrodynamic Equations of a Viscous Fluid in the Case of a Cylindrical Tube," Journal of Mathematical Pures et Appl., vol 11, pp 67-107, 1932.

13. P.J. Lefebvre and F.M. White, "Correlation of Transition to Turbulence in a Constant-Acceleration Pipe Flow," Forum on Turbulent Flows, ASME-FED, vol 51, 1987.

INITIAL DISTRIBUTION LIST

Addressee	No. of Copies
CNR (OCNR-11 (M. Reischman, S. Lekoudis), OCNR-12 (R. Fein), OCNR-20 (T. Remers))	5
NAVSEA (SEA-05 (A. Smookler), SEA-56W (P. Crabb), PMS-402)	4
DTRC, Carderock (D. Coder, L. Cathers)	2
DTIC	2
CNA	1